hanced nonradiative decay from the higher energy deactivating state is also explained by this model because intersystem crossing from the $E_u(^3E_u)$ state with respect to the lowest energy ($B_{1u}(^3E_u$, $B_{2u}(^3E_u)$) level will be promoted by the increased singlet character of the former state arising from efficient mixing with its energetically proximate singlet (vide supra). Moreover, the $E_u(^3E_u)$ state is possibly split by the Jahn-Teller effect and may therefore exhibit a larger nontotally symmetric distortion than the other spin-orbit states.[55] Such distortions are usually effective in promoting efficient nonradiative decay.

Thus, the excited-state dynamics of the $Pt^{III}_2(HPO_4)_4L_2^{n-}$ complexes clearly reveal the existence of efficient deactivation pathways of $d\sigma^*$ excited states even when metal-metal or metal-axial ligand dissociation is precluded. Our results suggest that the spin-orbit components of the $^3(d\pi^*d\sigma^*)$ configuration controls the dynamics of $d\sigma^*$ emission from the $Pt^{III}_2(HPO_4)_4L_2^{n-}$ complexes. Specifically, the $E_u(^3E_u)$ excited state proximate to the lowest energy emissive ($B_{1u}(^3E_u)$, $B_{2u}(^3E_u)$) level provides a facile decay channel to ground state. A small (B_{1u}, B_{2u}) - E_u energy gap may explain the absence of $d\sigma^*$ emission from other singly bonded metal-metal complexes. The ability to control the magnitude of this energy gap with heavy-atom donor ligands in the axial coordination sites provides the opportunity to synthetically tune the excited-state lifetime and, consequently, luminescence intensity of $d\sigma^*$ excited states.

Acknowledgment. We thank Drs. Al Stiegman and Mordechai Bixon for helpful discussions. The financial support of this work by National Science Foundation Grant CHE-8705871 (D.G.N.) is gratefully acknowledged.

Supplementary Material Available: Tables of temperature-dependent quantum yields, temperature-dependent lifetimes, and calculated radiative and nonradiative rate constants (3 pages). Ordering information is given on any current masthead page.

(55) Hopkins, M. D.; Miskowski, V. M.; Gray, H. B. *J. Am. Chem. Soc.* **1986**, *108*, 6908.

Contribution from the Department of Chemistry, Clemson University, Clemson, South Carolina 29634-1905

Competitive Hydrogen Production and Emission through the Photochemistry of Mixed-Metal Bimetallic Complexes

D. Brent MacQueen and John D. Petersen*

Received July 25, 1989

Preparation of the complexes $RhH_2(PPh_3)_2L^+$, $[RhH_2(PPh_3)_2]_2L^{2+}$, and $(bpy)_2RuLRhH_2(PPh_3)_2^{3+}$ where L is 2,2'-bipyrimidine (bpm), 2,3-bis(2-pyridyl)pyrazine (dpp), and 2,3-bis(2-pyridyl)quinoxaline (dpq), as well as the monometallic analogues $RhH_2(PPh_3)_2en^+$ and $RhH_2(PPh_3)_2bpy^+$ (en = ethylenediamine and bpy = 2,2'-bipyridine) is described. All of the complexes undergo photochemically induced reductive elimination of molecular hydrogen when irradiated at wavelengths equal to or shorter than 405 nm for the monometallic complexes and equal to or shorter than 436 nm for the bimetallic complexes. In addition, the monometallic rhodium complexes and the heterobimetallic (RuLRh) complexes undergo emission in fluid solution at room temperature from a state different than the photoactive state. In the case of the heterobimetallic complexes, the photoemissive state is best described as a Ru-based metal-to-ligand charge-transfer (MLCT) state while the photoreaction is assigned as a Rh-based ligand-field (LF) state in all of the complexes studied.

Introduction

The use of tris(bipyridine)ruthenium(II), $Ru(bpy)_3^{2+}$, as a photosensitizer has been widely exploited due to both the ion's inertness toward photosubstitution reactions and its long-lived excited state ($\tau \sim 600$ ns) at room temperature. In addition, the intense absorption feature that this complex displays in the visible region of the spectrum has made it a likely candidate for solar energy conversion studies.[2-5] $Ru(bpy)_3^{2+}$ has been used as an excited-state energy-transfer[6-9] as well as electron-transfer[10-14] reagent. The incorporation of a "$Ru(bpy)_3^{2+}$ like" chromophore into a multicomponent system to sensitize a useful photochemical reaction has been proposed in order to circumvent the inherent inefficiency of the bimolecular collision process used to facilitate energy or electron transfer in the previous photochemical systems.

Intramolecular energy transfer has been observed in numerous inorganic photochemical systems; however, most of the reported systems involve energy transfer from an intraligand transition (IL) to a ligand-field (LF) state from which photochemistry is observed.[15-17] The examples of energy transfer from a metal-to-ligand charge-transfer (MLCT) transition localized on one metal center to an LF or MLCT excited state of a covalently attached metal center are recent and few.[18-23]

The complexes $Ru(bpy)_2L^{2+}$ and $[Ru(bpy)_2]_2L^{4+}$, where L = 2,3-bis(2-pyridyl)pyrazine (dpp), 2,3-bis(2-pyridyl)quinoxaline

(1) Van Houten, J.; Watts, R. J. *J. Am. Chem. Soc.* **1976**, *98*, 4853.
(2) Kalyanasundaram, K. *Coord. Chem. Rev.* **1982**, *46*, 159.
(3) Kirch, M.; Lehn, J.; Sauvage, J. *Helv. Chim. Acta* **1979**, *62*, 1345.
(4) Juris, A.; Balzani, V.; Barigelletti, F.; Campagna, S.; Belser, P.; Von Zelewsky, A. *Coord. Chem. Rev.* **1988**, *84*, 85.
(5) Balzani, V., Ed. *Supramolecular Photochemistry*; NATO ASI Series C; D. Reidel: The Netherlands, 1987; Vol. 214.
(6) Lin, C.-T.; Böttcher, W.; Chou, M.; Creutz, C.; Sutin, N. *J. Am. Chem. Soc.* **1976**, *98*, 6536.
(7) Sabbatini, N.; Balzani, V. *J. Am. Chem. Soc.* **1972**, *94*, 7587.
(8) Demas, J. N.; Adamson, A. W. *J. Am. Chem. Soc.* **1971**, *93*, 1800.
(9) Kane-Maguire, N. A. P.; Langford, C. H. *J. Am. Chem. Soc.* **1972**, *94*, 2125.
(10) Navon, G.; Sutin, N. *Inorg. Chem.* **1974**, *13*, 2159.
(11) Gafney, H. D.; Adamson, A. W. *J. Am. Chem. Soc.* **1972**, *94*, 8238.
(12) Bock, C. R.; Meyer, T. J.; Whitten, D. G. *J. Am. Chem. Soc.* **1974**, *96*, 4710.
(13) Sutin, N.; Creutz, C. *Adv. Chem. Ser.* **1978**, *No. 168*, 1.
(14) Meyer, T. J. *Acc. Chem. Res.* **1978**, *11*, 94.
(15) Adamson, A. W.; Vogler, A.; Lantzke, I. *J. Phys. Chem.* **1969**, *73*, 4183.
(16) Bergkamp, M. A.; Watts, R. J.; Ford, P. C. *Inorg. Chem.* **1981**, *20*, 1764.
(17) Hennig, H.; Rehorek, D. *Coord. Chem. Rev.* **1985**, *61*, 1.
(18) Gelroth, J. A.; Figard, J. E.; Petersen, J. D. *J. Am. Chem. Soc.* **1979**, *101*, 3649.
(19) Moore, K. J.; Lee, L.; Figard, J. E.; Gelroth, J. A.; Stinson, A. J.; Wohlers, H. D.; Petersen, J. D. *J. Am. Chem. Soc.* **1983**, *105*, 2274.
(20) Nishizawa, M.; Ford, P. C. *Inorg. Chem.* **1981**, *20*, 2016.
(21) Schmehl, R. H.; Auerbach, R. A.; Wacholtz, W. F.; Elliott, C. M.; Freitag, R. A.; Merkert, J. W. *Inorg. Chem.* **1986**, *25*, 2440.
(22) Wacholtz, W. F.; Auerbach, R. A.; Schmehl, R. H. *Inorg. Chem.* **1987**, *26*, 2989.
(23) Schmehl, R. H.; Auerbach, R. A.; Wacholtz, W. F. *J. Phys. Chem.* **1988**, *92*, 6202.

0020-1669/90/1329-2313$02.50/0

(dpq), and 2,2′-bipyrimidine (bpm), have been studied previously

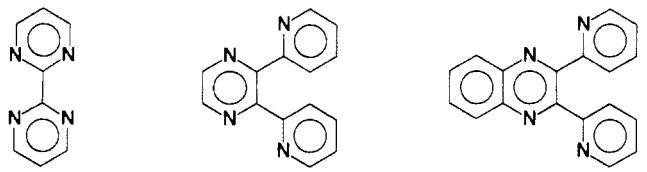

bpm dpp dpq

by our laboratory[24,25] and others[26-32] to determine their electrochemical and photophysical properties as well as the extent of metal–metal communication in the bimetallic complexes. These studies indicate that emission in the monometallic complexes is from an MLCT state involving primarily the π^* level associated with the bridging ligand (L). Luminescence data also indicate that even when excitation initially populates the Ru → bpy MLCT excited-state, the emission is still bridging ligand in nature. Electrochemical data on the homobimetallic complexes $[\{(bpy)_2Ru\}_2L]^{4+}$ indicate that the greatest degree of communication between metal centers is found when L = bpm while less interaction is observed when L = dpp or dpq.[25,32] This ordering in the bridging-ligand-dependent metal–metal interaction is consistent with emission quenching studies on the mixed-valence complexes, $[(CN)_4FeLRu(bpy)_2]^+$ (L = dpp and bpm).[33]

The photochemistry of complexes of the type $MH_2Cl(PPh_3)_3$ (M = Rh and Ir) have been studied by both Ford[34] and Geoffroy.[35] The early studies by Geoffroy indicated that the complex $RhH_2Cl(PPh_3)_3$ undergoes concerted reductive elimination of molecular hydrogen to give $RhCl(PPh_3)_3$. Ford's study supports the concerted mechanism in the rhodium complex, but in the iridium complex $IrH_2Cl(PPh_3)_3$, the primary process is the dissociation of a phosphine ligand to yield $IrH_2Cl(PPh_3)_2$, which subsequently undergoes thermal decomposition to produce molecular hydrogen.

The multicomponent photochemical system described in this work consists of three parts: a chromophore (based on $Ru(bpy)_3^{2+}$), which absorbs in the visible region of the spectrum, a bridging ligand capable of facilitating energy transfer, and a light-sensitive, reactive, metal complex fragment, (based on a rhodium(III) dihydride). The multicomponent design of this supramolecular complex should allow for flexibility in designing and modifying the various components of the system.

Experimental Section

Materials. All solvents used in complex preparation and photochemical experiments were reagent grade and used without further purification. HPLC grade acetone (Aldrich) was used in determining molar absorptivities and in all emission experiments.

Electrochemical experiments employed UV grade acetonitrile and spectrophotometric grade propylene carbonate (both from American Burdick and Jackson). Tetrabutylammonium hexafluorophosphate (TBAH) used as supporting electrolyte in all electrochemical experiments was prepared by metathesis of tetrabutylammonium bromide (Eastman) with HPF_6 (Alfa). The TBAH was then purified by recrystalling three times from ethanol.

The metal salts $RuCl_3 \cdot 3H_2O$ and $RhCl_3 \cdot 3H_2O$ were both obtained on loan from Johnson Matthey Inc. The ligands triphenylphosphine (PPh_3), ethylenediamine (en), 2,2′-bipyridine (bpy) and 2,3-bis(2-pyridyl)-pyrazine (dpp) were all obtained from Aldrich and used without further purification. The ligand 2,3-bis(2-pyridyl)quinoxaline was prepared according to the procedure described by Goodwin and Lions.[36] The ligand 2,2′-bipyrimidine (bpm) was obtained from Lancaster Synthesis and used without further purification. The KPF_6 salt used to precipitate complexes was obtained from Alfa Inorganics and used without further purification.

Syntheses. $[Ru(bpy)_2L](PF_6)_2$ (L = dpp, dpq, or bpm). Complexes of this type were prepared in a manner similar to that described by Hunziker and Ludi[26] for $[Ru(bpy)_2bpm](PF_6)_2$. Generally, a 2-fold excess of L was added to an aqueous ethanol solution of $Ru(bpy)_2Cl_2$[37] and the mixture heated at reflux for 6 h. The hexafluorophosphate salt was then obtained by the addition of a saturated aqueous solution of KPF_6.

The desired product was isolated from the reaction mixture by liquid chromatography. A 20 × 2.5 cm column of alumina (Fisher, 80–200 mesh) was developed with 2:1 acetonitrile–toluene as the mobile phase. The desired product elutes first, with higher molecular weight species left behind on the column.

$[RhH_2(PPh_3)_2L]PF_6$ (L = dpp, dpq, bpm, bpy, or en). These complexes were all prepared from the starting material $[RhH_2(PPh_3)_2(acetone)_2]^+$,[38] which was generated from $[Rh(PPh_3)_2NBD]^+$ (NBD = bicyclo[2.2.1]hepta-2,5-diene). In a typical experiment, 0.20 g (0.23 mmol) of $[Rh(PPh_3)_2NBD]PF_6$ was partially dissolved in 10 mL of acetone and treated with molecular hydrogen until a pale yellow solution was obtained. A 3-fold excess of dpp, 0.159 g (0.68 mmol), was then added and the volume reduced to ca. 3 mL under hydrogen. The addition of 10 mL of 100% ethanol caused the precipitation of the desired product as well as the homonuclear bimetallic complex $\{[Rh(PPh_3)_2H_2]_2dpp\}(PF_6)_2$, as shown by the cyclic voltammogram of the crude product. Increasing the ratio of L to rhodium did decrease the amount of bimetallic complex formed; however, there were no conditions observed that totally eliminated bimetallic products.

Separation of the desired product was afforded by liquid chromatography employing alumina (Fisher 80–200 mesh) as the stationary phase (20 × 2.5 cm) and acetone saturated with hydrogen as the mobile phase. A small purple band eluted first, followed by a yellow band, which was found to be the desired product. An orange-red band remained at the top of the column and was assumed to be the bimetallic complex. Previous experiments indicate that this type of compound decomposed on alumina; thus, collection and characterization of this band was not attempted. Typical yields in the synthesis of the monometallic rhodium complexes are in the range 40–60%.

$\{[RhH_2(PPh_3)_2]_2L\}(PF_6)_2$ (L = dpq, dpp, or bpm). This class of compound was prepared by a method similar to that of the mononuclear compounds with a ratio of L to rhodium of 1:3. Upon liberal washing with ethanol and recrystalization from acetone/ethanol, these complexes were obtained in pure form. Typical yields based on moles of L were in the 70–80% range.

$[(bpy)_2Ru(L)RhH_2(PPh_3)_2](PF_6)_3$ (L = dpp, dpq, or bpm). These complexes were all prepared by the addition of $[Ru(bpy)_2L](PF_6)_2$ to an acetone solution of $[RhH_2(PPh_3)_2(acetone)_2]PF_6$. If the ratio of Rh to Ru was kept greater than unity, the excess $[RhH_2(PPh_3)_2(acetone)_2]^+$ could be easily removed with liberal washings of ethanol. In fact, Osborn and Schrock[38] have shown that the actual complex formed when $[RhH_2(PPh_3)_2(acetone)_2]^+$ was dissolved in ethanol was $[RhH_2(PPh_3)_2(acetone)(ethanol)]^+$. In a typical experiment, 0.20 g (0.23 mmol) of $[Rh(PPh_3)_2NBD]PF_6$ was partially dissolved in 10–15 mL of acetone and bubbled with hydrogen until a pale yellow solution was obtained (~10 min). Then 0.20 g (0.21 mmol) of $[Ru(bpy)_2L](PF_6)_2$ was added and the volume reduced to 3 mL under hydrogen. The pure product was obtained by the addition of 100% ethanol, collected by vacuum filtration, and washed with liberal amounts of ethanol. Typically, 0.25 g of product was obtained, which corresponds to ~71% yield.

Instrumentation. Cyclic voltammetric experiments were carried out by using a EG & G Princeton Applied Research Model 273 potentiostat/galvanostat and an IBM Instrument Model 7424MT X-Y-T recorder. The cyclic voltammetric experiments employed a 2-mm platinum disk for both the working and auxiliary electrodes (Bioanalytical Sciences). The reference electrode was a saturated calomel electrode (SCE) with tetrabutylammonium hexafluorophosphate (TBAH) as the supporting electrolyte.

Emission spectra were obtained by using a SPEX Fluorolog II spectrometer controlled by a SPEX DM1B spectroscopy laboratory coordi-

(24) Petersen, J. D. In *Supramolecular Photochemistry*; Balzani, V., Ed.; NATO ASI Series C; D. Reidel: The Netherlands, 1987; Vol. 214, p 135.
(25) Wallace, A. W.; Murphy, W. R., Jr.; Petersen, J. D. Submitted for publication.
(26) Hunziker, M.; Ludi, A. *J. Am. Chem. Soc.* **1977**, *99*, 7370.
(27) Dose, E. V.; Wilson, L. J. *Inorg. Chem.* **1978**, *17*, 2660.
(28) Rillema, D. P.; Mack, K. B. *Inorg. Chem.* **1982**, *21*, 3849.
(29) Rillema, D. P.; Allen, G.; Meyer, T. J.; Conrad, D. *Inorg. Chem.* **1983**, *22*, 1617.
(30) Braunstein, C. H.; Baker, A. D.; Strekas, T. C.; Gafney, H. D. *Inorg. Chem.* **1984**, *23*, 857.
(31) Rillema, D. P.; Taghdiri, D. G.; Jones, D. S.; Keller, C. D.; Worl, L. A.; Meyer, T. J.; Levy, H. A. *Inorg. Chem.* **1987**, *26*, 578.
(32) Fuchs, Y.; Lofters, S.; Dieter, T.; Shi, W.; Morgan, R.; Strekas, T. C.; Gafney, H. D.; Baker, A. D. *J. Am. Chem. Soc.* **1987**, *109*, 2691.
(33) Wallace, A. W.; Petersen, J. D. Manuscript in preparation.
(34) Wink, D. A.; Ford, P. C. *J. Am. Chem. Soc.* **1986**, *108*, 4838.
(35) Geoffroy, G. L.; Pierantozzi, R. *J. Am. Chem. Soc.* **1976**, *98*, 8054.
(36) Goodwin, H. A.; Lions, F. *J. Am. Chem. Soc.* **1959**, *81*, 6415.
(37) Sullivan, B. P.; Salmon, D. J.; Meyer, T. J. *Inorg. Chem.* **1978**, *17*, 3334.
(38) Osborn, J. A.; Schrock, R. R. *J. Am. Chem. Soc.* **1971**, *93*, 2397.

nator. The spectra were plotted on a Houston Instruments DMP-40 digital plotter.

The light train used in photolysis experiments has been previously described.[39] Light intensities were measured by ferrioxalate actinometry.[40]

The hydrogen evolved in the continuous photolysis was determined on a GOW MAC model 550 gas chromatograph with a 6-ft × $^1/_8$-in. Analab Spherocarb column and a ReW thermal conductivity detector (80 mA). The injector port, column, and detector were all maintained at room temperature. High-purity argon (Linde) was used as the carrier gas with a metered flow rate of 40 mL/m. The instrument was calibrated by using a known concentration of hydrogen in argon. The chromatograms were recorded on a GOW MAC Model 70-750 strip chart recorder.

Photochemical experiments were carried out in 5-cm, dual-stoppered, quartz cells. One port was fitted with a gastight septum; the other was attached to a standard deoxygenation[41] flask. The deoxygenated, sample solution was introduced via a deoxygenation flask, and all undissolved gas was purged via a syringe placed just below the septum. After being checked for bubbles, the syringe was moved further into the cell and 500 mL of argon cover gas was introduced with the displacement of an equal volume of solution. The cell was then placed in the thermostated cell holder and irradiated for the desired photolysis time.

After photolysis, three 50-μL samples of the cover gas was injected into the gas chromatograph via a gastight syringe (Hamilton 1710). The signal intensity was then compared to the calibration curve, and the hydrogen concentration was determined. Knowing the total volume of gas in the cell and correcting for hydrogen dissolved in the acetone allowed the total number of moles of hydrogen evolved to be determined.

The same procedure was carried out with a cell maintained in the dark to determine any thermal contribution to the hydrogen yield. Any observed thermal contribution was subtracted from the total hydrogen evolved. The quantum yield for hydrogen production was determined from

$$\Phi_{H_2} = \frac{N}{I_0(1 - 10^{-\epsilon lc})(\Delta t)}$$

The total moles of H_2 evolved photochemically (N), the einsteins absorbed (I_0) from ferrioxalate actinometry, the photolysis time (Δt), and the fraction of incident light absorbed by the test solution at the wavelength of irradiation ($1 - 10^{-\epsilon lc}$) were used to calculate the quantum yield.

All electronic spectra were recorded on a Bausch and Lomb Spectronic 2000 instrument using matched quartz cells. Elemental analyses were determined by Atlantic Microlab, Inc., Atlanta, GA.

Results

Electronic Spectroscopy. The electronic spectral data and assignments of the three types of complexes studied in acetone are listed in Table I. In the case of the monometallic complexes, $[RhH_2(PPh_3)_2L]^+$, all species exhibit shoulders in the 360–410-nm region with the exception of the complex L = dpq, which exhibits a maximum at 370 nm (ϵ = 7.9 × 10^3 M^{-1} cm^{-1}) as well as a shoulder at 410 nm and the complex L = en, which is featureless in that spectral region. (The electronic spectrum of $RhH_2(PPh_3)_2dpp^+$ is shown in Figure 1.)

The homonuclear bimetallic complexes $[\{RhH_2(PPh_3)_2\}_2L]^{2+}$ display a single maxima in the 439–497-nm region with the complex L = dpq also exhibiting shoulders at 420 and 370 nm. The heteronuclear, bimetallic complexes $[(bpy)_2RuLRhH_2(PPh_3)_2]^{3+}$ (structure I shows an example for L = bpm[41]) all

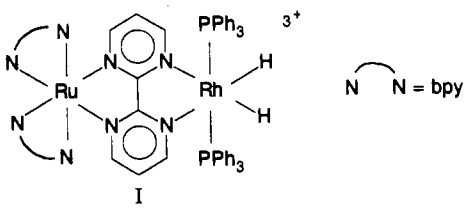

I

exhibit two maxima. A low-energy maximum is found in the 488–572-nm region while a higher energy maximum is found in the 397–425-nm region. (The electronic spectrum of $(bpy)_2Ru(dpp)RhH_2(PPh_3)_2^{3+}$ is shown in Figure 2.) Also, the complexes where L = dpq and bpm exhibit shoulders at 510 and 515 nm, respectively.

Table I. Electronic Absorption Spectra of Mono- and Bimetallic Complexes[a]

complex	λ_{max}, nm (ϵ_{max}, M^{-1} cm^{-1})[b] Rh → L MLCT[c]	IL[d]
$RhH_2(PPh_3)_2dpp^+$	380 (sh)	
$RhH_2(PPh_3)_2dpq^+$	410 (sh)	370 (7.9 × 10^3)
$RhH_2(PPh_3)_2bpm^+$	380 (sh)	
$RhH_2(PPh_3)_2bpy^+$	350 (sh)	
$RhH_2(PPh_3)_2en^+$	*e*	

complex	λ_{max}, nm (ϵ_{max}, M^{-1} cm^{-1}) Rh → L MLCT[c]	IL[d]
$[RhH_2(PPh_3)_2]_2(dpp)^{2+}$	439 (6.41 × 10^3)	
$[RhH_2(PPh_3)_2]_2(dpq)^{2+}$	497 (6.94 × 10^3), 420 (sh)	370 (sh)
$[RhH_2(PPh_3)_2]_2(bpm)^{2+}$	466 (2.37 × 10^3)	

complex	λ_{max}, nm (ϵ_{max}, M^{-1} cm^{-1}) M → L MLCT[c]	Ru → bpy MLCT
$[(bpy)_2Ru(dpp)RhH_2(PPh_3)_2]^{3+}$	488 (1.3 × 10^4)	425 (9.7 × 10^3)
$[(bpy)_2Ru(dpq)RhH_2(PPh_3)_2]^{3+}$	572 (1.3 × 10^4), 510 (sh)	397 (1.5 × 10^4)
$[(bpy)_2Ru(bpm)RhH_2(PPh_3)_2]^{3+}$	551 (4.9 × 10^3), 515 (sh)	413 (1.6 × 10^4)

complex	λ_{max}, nm (ϵ_{max}, M^{-1} cm^{-1}) Ru → L MLCT	Ru → bpy MLCT	Ru → L MLCT	IL
$Ru(bpy)_2dpp^{2+}$	465 (sh)	430 (1.3 × 10^4)		
$Ru(bpy)_2dpq^{2+}$	517 (8.9 × 10^3)	426 (9.2 × 10^3)	390 (sh)	350 (sh)
$Ru(bpy)_2bpm^{2+}$	424 (1.2 × 10^4)	395 (sh)	358 (8.3 × 10^3)	

[a] In acetone at 25 °C. [b] (sh) indicates a shoulder; molar extinction coefficients are accurate to ±5%. [c] Metal-to-ligand charge-transfer (MLCT) transition. [d] Internal ligand ($\pi \rightarrow \pi^*$) transition. [e] Onset of absorption is 380 nm, with continual rise into the ultraviolet region of the spectrum.

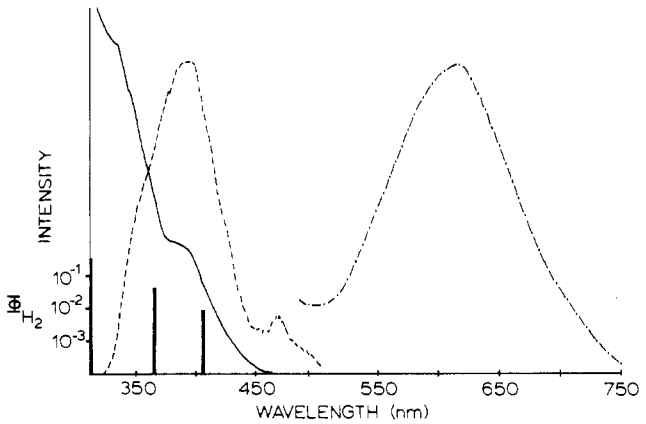

Figure 1. Absorption, excitation, and emission spectra of $RhH_2(PPh_3)_2dpp^+$ in acetone at room temperature. Overlayed on this plot are the log Φ_{H_2} values as a function of irradiation wavelength.

Electrochemistry. The cyclic voltammetric data for the rhodium complexes are given in Table II. The half-wave potential is $E_{1/2}$ (V), defined as

$$E_{1/2} = (E_{pc} + E_{pa})/2$$

where E_{pc} and E_{pa} are the peak cathodic and peak anodic potentials, respectively. The peak potential separation, ΔE (mV), is defined as

$$\Delta E = E_{pa} - E_{pc}$$

(39) Brewer, K. J.; Murphy, W. R.; Moore, K. J.; Eberle, E. C.; Petersen, J. D. *Inorg. Chem.* **1986**, *25*, 2470.
(40) Hatchard, C. G.; Parker, C. A. *Proc. R. Soc. London, A* **1956**, *235*, 518.
(41) MacQueen, D. B.; Pennington, W. T.; Petersen, J. D. Submitted for publication.

Table II. Electrochemical Studies of Mono- and Bimetallic Complexes[a]

complex	$E_{1/2}$ (ΔE)[b] $Ru^{III/II}$	$Rh^{IV/III}$	$L^{0/-}$	$L^{-/-2}$ and $bpy^{0/-}$
$RhH_2(PPh_3)_2dpp^+$		1.92 (E_a)	−1.26 (160)	
$RhH_2(PPh_3)_2dpq^+$		1.86 (E_a)	−1.03 (60)	−1.79 (120)
$RhH_2(PPh_3)_2bpm^+$		1.88 (E_a)	−1.34 (140)	−2.06 (E_c)
$RhH_2(PPh_3)_2bpy^+$		1.64 (E_a)		−1.64 (145)
$RhH_2(PPh_3)_2en^+$		1.57 (E_a)		
$[RhH_2(PPh_3)_2]_2dpp^{2+}$		1.89 (E_a)	−0.80 (80)	−1.50 (75)
$[RhH_2(PPh_3)_2]_2dpq^{2+}$		1.88 (E_a)	−0.58 (65)	−1.58 (90)
$[RhH_2(PPh_3)_2]_2bpm^{2+}$		1.90 (E_a)	−0.67 (55)	−1.53 (65)
$[(bpy)_2Ru(dpp)RhH_2(PPh_3)_2]^{3+}$	1.70 (120)	1.56 (E_a)	−0.66 (70), −1.28 (65), −1.51 (90), −1.73 (120)	
$[(bpy)_2Ru(dpq)RhH_2(PPh_3)_2]^{3+}$	1.71 (85)	1.56 (E_a)	−0.44 (70), −1.26 (70), −1.57 (75), −1.79 (90)	
$[(bpy)_2Ru(bpm)RhH_2(PPh_3)_2]^{3+}$		1.65 (E_a)[c]	−0.47 (70), −1.26 (70), −1.52 (90), −1.77 (105)	

[a] In acetonitrile with 0.1 M TBAH as supporting electrolyte. [b] $E_{1/2}$ (in V) vs SCE calculated as average of anodic and cathodic peaks with peak-to-peak separation (ΔE) shown in mV in parentheses. E_a or E_c in parentheses indicate that only the anodic or cathodic peaks were observed, respectively. [c] The reported E_a value is this combination of overlapping anodic waves for Ru(I) and Rh(III).

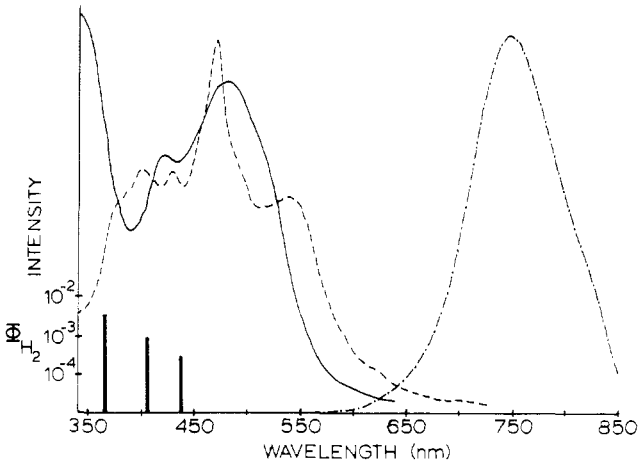

Figure 2. Absorption, excitation, and emission spectra of $(bpy)_2Ru(dpp)RhH_2(PPh_3)_2^{3+}$ in acetone at room temperature. Overlayed on this plot are the log Φ_{H_2} values as a function of irradiation wavelength.

All potential values reported are versus a saturated calomel electrode (SCE).

The reversibility of a redox process is determined by the shape and position of both waves, cathodic and anodic, of the redox couple. If $i_{pa} \approx i_{pc}$ (where i_{pa} and i_{pc} are the peak anodic and cathodic currents, respectively), then the redox couple is termed chemically reversible. Redox couples are also described as exhibiting Nernstian[42] behavior when $\Delta E \approx 60$ mV and $i_p \propto v^{1/2}$ (where i_p is the peak current and v is the scan velocity in V/s).

The cyclic voltammograms obtained with an initial anodic scan for all monometallic complexes studied, $RhH_2(PPh_3)_2L^+$, exhibit a single irreversible redox process. The redox process is irreversible, as only an anodic wave with no cathodic counterpart is observed. For the complexes with L = dpq, dpp, and bpm, the anodic wave is observed in the 1.86–1.92-V (vs SCE) region while the complexes L = bpy and en display anodic waves at 1.64 and 1.57 V (vs SCE), respectively.

The voltammograms obtained in the negative scan exhibit redox properties covering a wider potential range with varying degrees of reversibility. All three complexes $[RhH_2(PPh_3)_2L]^+$ (L = dpp, dpq, and bpm) show a chemically reversible redox process, $L^{0/-}$, in the −1.03- to −1.34-V (vs SCE) region; however, only in the case of L = dpq does the redox process exhibit Nernstian behavior. The compound L = dpq and bpm both show a second bridging ligand reduction, $L^{-/2-}$. The compound L = bpm displays a cathodic wave, with no anodic counterpart, at −2.06 V while the compound L = dpq displays a redox process with $E_c = -1.79$ V, which exhibits irreversible Nernstian behavior but appears to be chemically reversible.

The homonuclear bimetallic complexes, $[\{RhH_2(PPh_3)_2\}_2L]^{2+}$ (where L = dpp, dpq, or bpm), exhibit the same anodic behavior as was observed in the monometallic complexes $[RhH_2(PPh_3)_2L]^+$. The irreversible rhodium oxidations (no cathodic counterpart observed) occur at 1.89, 1.88, and 1.90 V (vs SCE) for the L = dpp, dpq, and bpm complexes, respectively. Upon repeated cycling, the peak potential shifted in a random fashion by as much as 20 mV with the current remaining essentially constant. Coulometric determination of the number of electrons involved in the oxidation was not attempted due to the irreversible nature of the process. Thus whether the oxidation involves one or both metal centers is not apparent although within the solvent window (+2.2 V) only a single anodic wave is observed.

All three rhodium homonuclear bimetallic complexes, $[RhH_2(PPh_3)_2]_2L^{2+}$ (L = bpm, dpp and dpq) exhibit two waves in the cathodic scan. These redox processes are assigned as sequential, one-electron reductions of the bridging ligand, i.e., $L^{0/-}$ and $L^{-/2-}$. The least negative redox couples are found in the −0.58 to −0.80 V (vs SCE) range. The complexes L = dpq, $E_{1/2} = -0.58$ V ($\Delta E = 65$ mV), and L = bpm, $E_{1/2} = -0.67$ V ($\Delta E = 55$ mV), exhibit Nernstian behavior while the compound L = dpp, $E_{1/2} = -0.80$ V ($\Delta E = 75$ mV), is chemically reversible but only quasi-reversible in the Nernstian sense.

The most negative waves lie in a much narrower potential range, −1.50 to −1.58 V, than the previously described waves. All three redox processes are chemically reversible, however; in the Nernstian sense, the complexes L = dpq, dpp, and bpm are reversible, quasi-reversible, and irreversible, respectively.

The electrochemistry observed for the series of heterobimetallic compounds $[(bpy)_2RuLRhH_2(PPh_3)_2]^{3+}$ (L = dpp, dpq, and bpm) is very rich. The anodic scan exhibits two oxidations while the cathodic scan shows four reductions. In the positive scan, the two redox processes are distinguishable with the exception of those for the L = bpm complex in which the two processes overlap such that only one anodic wave is observed. In the L = dpp and dpq complexes, the more positive process does exhibit both anodic and cathodic waves although overlap with the anodic wave of the other redox process prohibits any determination of reversibility.

In the cathodic scan, four redox couples are observed, all of which appear to be chemically reversible; however, only the first two redox couples in all of the $[(bpy)_2RuLRhH_2(PPh_3)_2]^{3+}$ complexes behave in a Nernstian manner.

Emission Spectroscopy. The room-temperature emission maxima, quantum yields,[43] lifetime measurements, and excitation spectra maxima and assignments are given in Table III. An

(42) Bard, A. J.; Faulkner, L. R. *Electrochemical Methods, Fundamentals and Applications*; John Wiley and Sons, Inc.: New York, 1980.

(43) Hager, G. D.; Crosby, G. A. *J. Am. Chem. Soc.* **1975**, *97*, 7031.

Table III. Emission and Excitation Spectra of Mono- and Bimetallic Complexes[a]

complex	λ_{max}^{ex} [b]	λ_{max}^{em} [c]	Φ_{em} [d]	τ [e]	assignt [f]
$RhH_2(PPh_3)_2dpp^+$	388	649	3.6×10^{-5}	~30	dpp → Rh
$RhH_2(PPh_3)_2bpm^+$	389	630	5.0×10^{-4}	<20	bpm → Rh
$RhH_2(PPh_3)_2bpy^+$	365	593	3.2×10^{-5}	<20	bpy → Rh
$[(bpy)_2Ru(dpp)$-$RhH_2(PPh_3)_2]^{3+}$	537	776	9.2×10^{-3}	106	dpp → Ru
$[(bpy)_2Ru(bpm)$-$RhH_2(PPh_3)_2]^{3+}$	467 546 sh	767	1.9×10^{-3}	41	bpm → Ru
$Ru(bpy)_2dpp^{2+}$	466	663	5.1×10^{-2}	113	dpp → Ru
$[Ru(bpy)_2]_2dpp^{4+}$	469	769	3.1×10^{-3}	54	dpp → Ru

[a] In acetone at 25 °C. [b] Maximum (in nm) of excitation spectrum while monitoring at λ_{max}^{em}. [c] Emission maximum (in nm). [d] Quantum yield for emission, calculated by using the method reported by: Hager, G. D.; Crosby, G. A. *J. Am. Chem. Soc.* **1975**, *97*, 7031. [e] Excited-state lifetime (in ns). [f] Assignment for the originating and final orbitals for the electron involved in the emission from the MLCT state.

emission is observed in the complexes $RhH_2(PPh_3)_2L^+$ (L = bpm, dpp, or bpy) and $(bpy)_2RuLRhH_2(PPh_3)_2^{3+}$ (L = bpm or dpp) while no emission is observed for any of the complexes with dpq as a ligand or any of the homonuclear bimetallic complexes $[RhH_2(PPh_3)_2]_2L]^{2+}$.

In all complexes, there is a distortion in the low-energy region of the corrected emission spectra due to the errors in correcting for photomultiplier tube response at the red limit. Since this distortion made it difficult to integrate the emission curve for quantum yield calculations, an alternate method was used. Initially, the spectrum was converted to an energy scale by changing the x axis from nm to cm^{-1}. The quantum yield was calculated by measuring the area from the high-energy tail of the emission to the observed maxima and then multiplying this value by 2.

The $RhH_2(PPh_3)_2L^+$ complexes with L = bpm, dpp, or bpy exhibit emission spectra with an emission maximum (excitation wavelength) of 630 nm (389 nm), 649 nm (388 nm), and 593 nm (365 nm), respectively (see Figure 1 for dpp complex). The observed emission quantum yields, Φ_{em}, are 5.0×10^{-4}, 3.6×10^{-5}, and 3.2×10^{-5} for L = bpm, dpp, and bpy, respectively. The emission lifetimes are near the limit of detection of our system (~20 ns) but appear to be approximately 30 ns for the $RhH_2(PPh_3)_2dpp^+$ complex while the bpm and bpy analogues have lifetimes less than 20 ns. The excitation spectra shows that the shoulder at ~380 nm in the absorption spectra is the transition that leads to the observed emission.

The $(bpy)_2RuLRhH_2(PPh_3)_2^{3+}$ complexes with L = bpm or dpp exhibit emission spectra with a maximum (excitation maximum) of 767 nm, with a shoulder at 546 nm (467 nm), or 776 nm (537 nm), respectively (see Figure 2 for dpp complex). The observed quantum yields (lifetimes) are 1.9×10^{-3} (41 ns) and 9.2×10^{-3} (106 ns) for L = bpm and dpp, respectively. The excitation spectra maxima occurs at 467 nm for the bpm- and 537 nm for the dpp-bridged species.

Photochemistry. All three classes of rhodium hydride complexes studied, the monometallic, homonuclear bimetallic, and heteronuclear bimetallic, undergo reductive elimination of molecular hydrogen in acetone at excitation wavelengths of 405 nm and shorter. The bimetallic complexes, both homo- and heteronuclear, display this behavior at an excitation wavelength of 436 nm as well. The quantum yields for the reductive elimination of hydrogen, Φ_{H_2}, at all excitation wavelengths used are given in Table IV.

Typically, the quantum yields are larger for irradiation at 365 nm than at the longer wavelengths. Additionally the quantum yields generally are highest for the monometallic Rh complexes, intermediate for the homonuclear bimetallic Rh complexes, and smallest for the heteronuclear bimetallic Ru/Rh analogues.

Within a given series of complexes, the quantum yields decrease in the order dpq > dpp > bpm > bpy, en. The exception in this trend is $RhH_2(PPh_3)_2bpm^+$, which has the largest quantum yield of all of the rhodium monometallic complexes at an irradiation wavelength of 405 nm. Within the series of monometallic and bimetallic complexes, the quantum yields are dependent on the nature of the complex (i.e., monometallic, homobimetallic, or heterometallic) and the irradiation wavelength, but are reasonably insensitive to the nature of L.

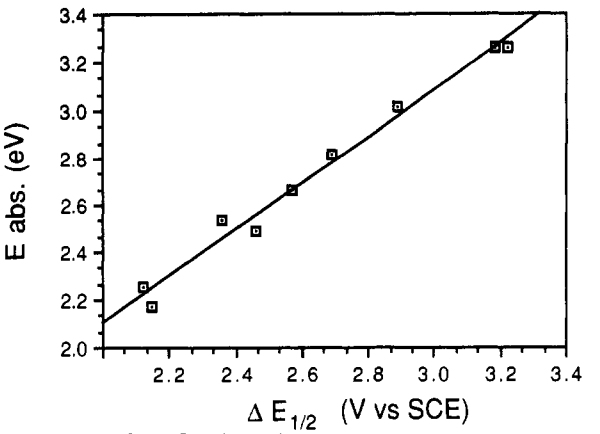

Figure 3. Plot of MLCT absorption maximum vs $\Delta E_{1/2}$.

Discussion

The assignment of the observed electronic absorption or shoulders in the case of the monometallic complexes is based on the well-established correlation between metal-to-ligand charge-transfer (MLCT) transition energies and the energy difference between the metal oxidation and the first ligand reduction.[4,44,45] Thus, a plot of the MLCT absorption energy (eV) and the difference between redox couples (V) should be linear with unity slope. As shown in Figure 3, such a plot has a correlation coefficient of 0.98 and a slope of 0.89. The presence of more than one absorption maxima and metal oxidation for some complexes leads to some deviation from the expected linearity in Figure 3.

The observed shoulders in the monometallic complexes are assigned as MLCT transitions based upon the above-mentioned correlation. Further evidence for this assignment is found in the lack of a shoulder in the complex $RhH_2(PPh_3)_2en^+$. If the shoulder was due to a ligand-field (LF) transition, then we would expect the en complex to exhibit a shoulder as well. The possibility of the shoulder being due to an intraligand ($\pi \rightarrow \pi^*$) transition can easily be ruled out due to the relatively low molar absorptivity in this spectral region. The maximum in the complex $RhH_2(PPh_3)_2dpq^+$ at 370 nm ($\epsilon = 7.9 \times 10^3$) is assigned to such an intraligand ($\pi \rightarrow \pi^*$) transition.

Previous studies[26-28,30,32] have shown that MLCT transitions associated with the bridging ligands employed in this study undergo a red shift when the ligands are coordinated to two metal centers relative to the same ligands coordinated to a single metal center. From the correlation of absorption and redox energies and the trend mentioned above, the assignment of the band observed in the 430–500-nm region as an MLCT transition seems appropriate.

As stated in the electrochemistry discussion, the first oxidation involves the rhodium while the first reduction involves the bridging ligand. On the basis of these observations the assignment of the low-energy band would be as a Rh → BL MLCT transition. However, the $Ru^{III/II}$ couple is very close to the rhodium oxidation ($\Delta E \sim 0.14$ V), and in fact, the overlap in the L = bpm complex is such that only one anodic wave is reported.

Close inspection of the low-energy band in the L = bpm and L = dpq complexes reveals a shoulder in the 510–515 nm spectral region, while the L = dpp complex has a low-energy maximum in that region. Thus, we feel the correct assignment of these low-energy bands involves an overlap of two MLCT transitions with the Rh → L transition occurring at slightly lower energy than the Ru → L transition. A comparison of the magnitude of the extinction coefficients observed for the Rh/Rh system to those of the Ru/Rh system (Table I) suggests that the Ru → L MLCT

(44) Vlček, A. A. *Electrochim. Acta* **1968**, *13*, 1063.
(45) Ohsawa, Y.; Hanck, K. W.; DeArmond, M. K. *J. Electroanal. Chem. Interfacial Electrochem.* **1984**, *175*, 229-240.

Table IV. Photochemical Quantum Yields of Mono- and Bimetallic Complexes[a]

complexes	Φ_{H_2}[b] at 436 nm	at 405 nm	at 365 nm
$RhH_2(PPh_3)_2dpp^+$		$(8.5 \pm 1.9) \times 10^{-3}$	$(4.0 \pm 0.6) \times 10^{-2}$[c]
$RhH_2(PPh_3)_2dpq^+$		$(1.5 \pm 0.1) \times 10^{-2}$	$(6.0 \pm 1.2) \times 10^{-2}$
$RhH_2(PPh_3)_2bpm^+$		$(2.1 \pm 0.1) \times 10^{-2}$	$(4.0 \pm 0.6) \times 10^{-2}$
$RhH_2(PPh_3)_2bpy^+$		$(4.4 \pm 0.6) \times 10^{-3}$	$(1.0 \pm 0.2) \times 10^{-2}$
$RhH_2(PPh_3)_2en^+$		$(4.3 \pm 1.0) \times 10^{-3}$	$(1.7 \pm 0.4) \times 10^{-2}$
$[RhH_2(PPh_3)_2]_2dpp^{2+}$	$(1.6 \pm 0.1) \times 10^{-3}$	$(6.1 \pm 0.3) \times 10^{-3}$	$(2.9 \pm 0.4) \times 10^{-2}$
$[RhH_2(PPh_3)_2]_2dpq^{2+}$	$(3.6 \pm 0.3) \times 10^{-3}$	$(1.1 \pm 0.3) \times 10^{-2}$	$(1.6 \pm 0.2) \times 10^{-2}$
$[RhH_2(PPh_3)_2]_2bpm^{2+}$	$(2.2 \pm 0.6) \times 10^{-4}$	$(1.2 \pm 0.2) \times 10^{-3}$	$(4.8 \pm 0.4) \times 10^{-3}$
$[(bpy)_2Ru(dpp)RhH_2(PPh_3)_2]^{3+}$	$(3.0 \pm 0.5) \times 10^{-4}$	$(9.4 \pm 0.4) \times 10^{-4}$	$(3.6 \pm 1.4) \times 10^{-3}$
$[(bpy)_2Ru(dpq)RhH_2(PPh_3)_2]^{3+}$	$(1.0 \pm 0.1) \times 10^{-3}$	$(6.1 \pm 0.3) \times 10^{-3}$	$(8.5 \pm 0.2) \times 10^{-3}$
$[(bpy)_2Ru(bpm)RhH_2(PPh_3)_2]^{3+}$	$(1.6 \pm 0.3) \times 10^{-4}$	$(2.1 \pm 0.2) \times 10^{-4}$	$(1.0 \pm 0.4) \times 10^{-3}$

[a] In acetone at 25 °C. [b] Quantum yield for production of H_2 reported (in mol/einstein) as a function of irradiation wavelength with the average deviation of at least 9 (and as large as 15 in some cases) independent trials listed. [c] Quantum yield at 313-nm irradiation in ethanol is 1.3×10^{-1} mol/einstein.

transition will dominate the spectral region of interest.

The high-energy bands located in the 397–425-nm region of the spectrum for all of the heterobimetallic complexes are assigned as Ru → bpy MLCT transitions. This assignment is based on the lack of dependence of the band maxima on the nature of the bridging ligand as well as a resonance Raman study by Gafney et al.[30] on the $[Ru(bpy)_2]_2dpp^{4+}$ ion. In this study,[30] they observed that 425-nm Raman excitation resulted in resonance enhancement of bpy vibrations. They also showed that excitation of the dpp-bridged ruthenium complex at 514.5 nm resulted in resonance enhancement of vibrations associated with the dpp bridging ligand. Thus, the current and previous studies are all consistent with the assignment of the high-energy bands as being Ru → bpy MLCT transitions but to the assignment of the lower energy bands as a M → BL (M = Ru(II), Rh(III)) MLCT mixed-metal transition.

Electrochemistry. The assignment of redox couples is based on previously observed behavior of d^6 metal complexes employing polypyridyl ligands.[46,47] Typically, a redox couple observed in the cathodic scan is associated with a ligand-centered reduction while a wave observed in the anodic scan is associated with a metal-centered oxidation.

The cyclic voltammograms obtained with an initial anodic scan exhibit a wave in the 1.86–1.92-V region for the complexes $[RhH_2(PPh_3)_2L]^+$ (L = bpm, dpp, and dpq). The lack of a corresponding cathodic wave when the potential sweep is reversed indicates that the rhodium oxidation is an electrochemically irreversible process. Due to the irreversible nature of this oxidation, coulometric determination of the number of electrons involved in the process was not attempted and the oxidation state initially formed is not known. We speculate that the oxidation involves formation of a Rh(IV) complex, which then undergoes an unknown chemical reduction process to re-form a Rh(III) species. While the oxidation to Rh(IV) is speculative, the subsequent chemical reduction to Rh(III) is apparent because the anodic current remains constant after repeated cycling of the potential through the electrochemically irreversible oxidative process. The reduction of the oxidation product is chemical in nature because no cathodic current is observed during the cycling process.

The anodic shift in the first bridging ligand reduction of the homonuclear bimetallic complexes relative to that of the monometallic complexes is consistent with observations others have made. For example, when the $Ru(bpy)_2L^{2+}$ vs $[Ru(bpy)_2]_2L^{4+}$ series of complexes are compared, the shift in potential is typically ~400 mV.

The assignment of the second reduction in the homonuclear bimetallic complexes as being $L^{-/2-}$ is based on the relative separation of the reductions. In the mononuclear complexes, $RhH_2(PPh_3)_2L^+$ (L = dpq and bpm), two reductions are observed, separated by 700 mV. In the homonuclear bimetallic complexes, the two BL reductions are separated by approximately the same amount. This assignment is also based on the cyclic voltammogram of the complex $[Ru(phen)_2]_2L^{4+}$, which will be discussed when the reductions in the heteronuclear, bimetallic complexes are assigned.

Gafney et al.[30] have proposed that the amount of shift in the first oxidation of a bimetallic complex relative to the oxidation of the monometallic complex is indicative of the extent of metal–metal interaction. When this comparison is made in the series $[Ru(bpy)_2]_2L^{4+}$ and $Ru(bpy)_2L^{2+}$ (where L = dpp, dpq and bpm), only the bpm bimetallic complex showed any substantial shift (0.17 V) while the dpq and dpp complexes shift only by 0.06 and 0.01 V, respectively. Thus, from Gafney's criteria for the extent of metal–metal interaction,[30] only the bpm bimetallic complex exhibits any considerable interaction.

In the case of the bimetallic rhodium complexes, only a 0.02–0.03-V shift is observed in any complex. The small amount of shift in oxidation potential implies weak metal–metal interaction at best. This brings up the question of why the bpm bridging ligand affords metal–metal interaction in the ruthenium complexes but does not appear to in the rhodium complexes. A possible explanation has to do with the energetics of the HOMO's involved. From our electrochemical results, the energy of the HOMO in the rhodium monometallic complex, $RhH_2(PPh_3)_2bpm^+$, is 0.52 V (4200 cm^{-1}) lower in energy than the HOMO of $Ru(bpy)_2bpm^{2+}$. Thus, the interaction between the metal orbitals is not as large in the dirhodium system due to poorer energy match and overlap of the metal HOMO ($d\pi$) with the ligand LUMO (π^*).

In the heteronuclear bimetallic complexes $(bpy)_2RuLRhH_2(PPh_3)_2^{3+}$, two oxidations are observed when scanning is performed anodically. The least positive process is an irreversible oxidation characteristic of the previously described rhodium complexes; i.e., no cathodic wave is observed. Thus this least positive oxidation is assigned as a rhodium oxidation while the more positive redox couple is assigned as $Ru^{III/II}$ on the basis of its displaying both an anodic and cathodic wave.

The most positive of the reduction couples displays a considerable variation in potential, $-0.44\ V \geq E_{1/2} \geq -0.66\ V$ ($\Delta E_{1/2}$ = 220 mV), as the bridging ligand is varied. This behavior and the previously reported behavior of the same bridging ligands[24,48,49]

(46) (a) Tokel-Takvoryan, N. E.; Hemingway, R. E.; Bard, A. J. *J. Am. Chem. Soc.* **1973**, *95*, 6582. (b) Kew, G.; DeArmond, H. K.; Hanck, K. *J. Phys. Chem.* **1974**, *78*, 727. (c) Kew, G.; DeArmond, H. K.; Hanck, K. *J. Phys. Chem.* **1975**, *79*, 1828. (d) Saji, T.; Aoyagui, S. *J. Electroanal. Chem. Interfacial Electrochem.* **1975**, *58*, 401. (e) Saji, T.; Yamada, T.; Aoyagui, S. *J. Electroanal. Chem. Interfacial Electrochem.* **1975**, *61*, 147.

(47) (a) Motten, A. G.; Hanck, K. W.; DeArmond, M. K. *Chem. Phys. Lett.* **1981**, *79*, 541. (b) Morris, D. E.; DeArmond, M. K.; Hanck, K. W. *J. Am. Chem. Soc.* **1983**, *105*, 3032. (c) Elliott, C. M.; Hershenhart, E. J. *J. Am. Chem. Soc.* **1983**, *105*, 3032. (d) Angel, S. M.; DeArmond, M. K.; Donohoe, R. J.; Hanck, K. W.; Wertz, D. W. *J. Am. Chem. Soc.* **1984**, *106*, 3688. (e) Tait, C. D.; MacQueen, D. B.; Donohoe, R. J.; DeArmond, M. K.; Hanck, K. W.; Wertz, D. W. *J. Phys. Chem.* **1986**, *90*, 1766.

(48) Brewer, K. J.; Murphy, W. R., Jr.; Spurlin, S. R.; Petersen, J. D. *Inorg. Chem.* **1986**, *25*, 882.

in other bimetallic complexes leads to the most positive reduction being assigned as $L^{0/-}$. The remaining three redox couples can be assigned as a $L^{-/2-}$ or $bpy^{0/-}$ ligand reductions.

The complexes $[Ru(phen)_2]_2L^{4+}$ have been shown to exhibit two sequential one-electron reductions, at $-0.40 > E_{1/2}(1) > -0.64$ and $-1.09 > E_{1/2}(2) > -1.13$ V vs SCE, before the onset of absorption waves characteristic of the reduction of coordinated phenanthroline.[45a] Also the two more negative redox couples are very similar to the second and third reduction potentials observed in a number of $Ru(bpy)_2L^{2+}$ complexes.[48,49] On the basis of the above observations, the reductions observed in the range -1.26 to -1.28 V (vs SCE) are assigned as $L^{-/2-}$ while the two more negative reductions are assigned as $bpy^{0/-}$.

Emission Spectra. The monometallic Rh(III) complexes display room-temperature emission spectra only for L = bpy, dpp, and bpm. These results are consistent with the assignment of an MLCT excited-state ($\pi^* \rightarrow$ Rh) based emission given the assignments of the absorption bands and the ~390 nm maximum for these systems in the excitation spectrum. The lack of emission observed for L = dpq can be rationalized by considering the energy of the excited state. If the dpp and dpq systems are compared, the latter has an MLCT absorption maximum that is shifted by ~0.2 μm^{-1} from the former. A corresponding shift of the emissive states may lead to a ground-/excited-state gap for L = dpq that is small enough to enable a facile deactivation to the ground state or at least small enough to be past the red-sensitive end of our detector (~850 nm). In the case of $RhH_2(PPh_3)_2en^+$, there is no low-lying π^* state associated with en and thus emission from an MLCT excited state cannot occur.

The homobimetallic complexes $[RhH_2(PPh_3)_2]_2L^{2+}$ do not display room-temperature emission. The coordination of the second Rh(III) metal center to L stabilizes the π and π^* levels in L, leading to lower energy MLCT states. This is observed in absorption where the monometallic complexes have MLCT maxima in the 380-nm region while the bimetallic complexes absorb at ≥440 nm. This red shift in absorption would carry over to the energy gap between the ground and lowest excited states in these systems and make the energy gap too small (i.e., lifetime too short) for emission to be observed at room temperature.

The heterobimetallic complexes $(bpy)_2RuLRhH_2(PPh_3)_2^{3+}$ undergo emission when L = dpp or bpm but not for L = dpq. Once again, a small ground-/excited-state energy gap can be used to rationalize the dpq data. In the case of L = dpp and bpm, the emissions are centered around 770 nm (Table III) and excitation spectra show maxima at approximately 540 nm. In addition, the excited-state lifetimes are much longer than those observed for the monometallic Rh(III) species. These data are similar to the results observed for the ruthenium mono- and bimetallic complexes (Table III) and suggest that the emissions observed in the heterobimetallic complexes are ruthenium MLCT excited-state-based emissions.

When the lifetimes in the heterobimetallic complexes are compared, the dpp bridged system at 106 ns is longer lived than the bpm system at 41 ns. This is consistent with the relative communicating abilities of the bridging ligands.[24,25,30,49] The bpm bridging ligand electronically couples the Ru and Rh metal centers to a greater extent, thus allowing the Rh center to assist in the deactivation of the Ru-based excited state.

Photochemistry. The primary photochemical process observed for all complexes reported in this work (i.e., monometallic rhodium, bimetallic rhodium, and heterobimetallic ruthenium/rhodium) is the reductive elimination of molecular hydrogen. That the hydrogen is evolved via a reductive-elimination process is confirmed by the cyclic voltammogram of the photoproduct, which shows a wave typical of a four-coordinate, Rh(I) oxidation. The photoreaction in all cases is irreversible as treatment of the photoproduct with molecular hydrogen did not result in regeneration of the starting material.

(49) Wallace, A. W. Ph.D. Dissertation, Clemson University, 1988.

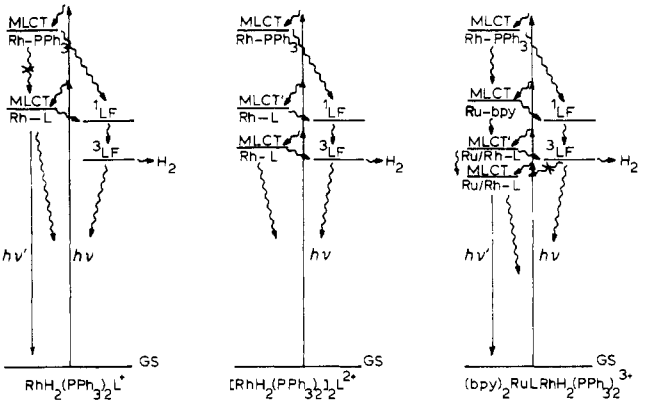

Figure 4. Proposed energy level diagrams for (a, left) $RhH_2(PPh_3)_2L^+$, (b, center) $[RhH_2(PPh_3)_2]_2L^{2+}$, and (c, right) $(bpy)_2RuLRhH_2(PPh_3)_2^{3+}$.

The magnitude of Φ_{H_2} at excitation wavelengths of 405 and 365 nm follows the trend

$$RhH_2(PPh_3)_2L^+ > RhH_2(PPh_3)_2L'^+ \simeq [RhH_2(PPh_3)_2]_2L^{2+} > (bpy)_2RuLRhH_2(PPh_3)_2^{3+}$$

L = bpm, dpp, dpq; L' = bpy, en

At 436 nm, the dirhodium system has a higher quantum yield than the ruthenium/rhodium system. As a general trend for all of the complexes, Φ_{H_2} increases with increasing energy of excitation.

In Figure 1, the values for log Φ_{H_2} for the complex $RhH_2(PPh_3)_2dpp^+$ are superimposed on the absorption, excitation, and emission spectra of the same complex. While the excitation spectrum clearly shows that the emission comes from excitation of the shoulder at 380 nm (i.e., Rh → dpp, MLCT), the H_2 production quantum yield does not follow the same profile. Therefore, we would not expect photochemistry and photophysics to come from the same excited state. Considering that all of the rhodium systems, including L = en, photochemically produce H_2, this rules out a Rh → L MLCT state or an IL state on L as the state responsible for the photochemistry. The most likely explanation is that photochemistry is occurring from a ligand field (LF) state on the rhodium center, although the participation of the Rh → PPh_3 MLCT cannot be eliminated from consideration.

The profile of the excitation spectrum in Figure 1 shows a return toward the base line at ~330 nm. Since this reduction in intensity of the excitation spectrum at higher energies occurs in ethanol as well as acetone, it can not be due to solvent cutoff in acetone. The failure of the excitation spectrum to follow the absorption spectrum indicates a lack in the ability to convert from the photoactive to the photoemissive state. On the other hand, photochemistry is observed throughout the spectrum, suggesting that the conversion from photoemissive to photoactive states is possible. The simplest schematic explaining this behavior is illustrated in Figure 4. Irradiation into any major absorption feature (i.e., MLCT transition) leads to H_2 production from ^{3}LF. However, emission only occurs when the Rh → L MLCT band is irradiated due to a lack of the ability of the Rh → PPh_3 MLCT or the ^{1}LF state to interconvert to the emissive state.

The same type of diagram and arguments presented for L = dpp in Figures 1 and 4a can be used for L = bpm, dpq, and bpy. However, for L = bpy, the photochemistry and photophysics are much lower in efficiency. This is apparently due to a shortening of the lifetime of the complex and is not a consequence of smaller radiative and reactive rate constants although we have no explanation for this behavior at this time.

The homobimetallic complexes $[RhH_2(PPh_3)_2]_2L^{2+}$ (L = dpp, dpq and bpm) produce H_2 photochemically at 436, 405, and 365 nm. None of the complexes display room-temperature emission as do the monometallic analogues. The loss of emission is probably the result of the introduction of an additional Rh → L MLCT state and the red shift of the entire MLCT manifold (Figure 4b). This shift to lower energy generates a smaller energy gap between ground and excited states that facilitates the nonradiative deactivation process. There should be little change in the energy of

the ligand-field manifold upon complexation of a second Rh(III) metal center. The shift to lower energy of the charge-transfer manifold extends the threshold irradiation wavelength used to generate H_2 from 405 and 436 nm. Apparently, internal conversion to the photoactive state is competitive with nonradiative decay to the ground state in these complexes, but emission is not a competitive process.

The heterobimetallic complexes $(bpy)_2RuLRhH_2(PPh_3)_2^{3+}$ display competitive emission and photochemistry, but in a unique manner. The photochemistry is the photoelimination from a Rh(III)-based excited state with threshold excitation energies that are the same as those for the dirhodium system. However, as pointed out in an earlier section, the emission is characteristic of a ruthenium-based MLCT. In Figure 2, the absorption, excitation, and emission spectra are overlayed on the same diagram. Once again, the excitation profile approaches the base line at higher energies, indicating that upper excited states can bypass the emissive state during interconversion/intersystem crossing back to the ground state. The photochemical quantum yields also illustrated in Figure 2 indicate that the lowest MLCT state is not capable of populating the photoactive state (see Figure 4c). While the lowest MLCT state is presumed to be a M → L MLCT state where M has substantial Ru(II) character on the basis of the emission spectrum and lifetime, the similarity in potential for Ru(II) and Rh(III) oxidations would suggest that the d orbitals are close in energy and thus capable of mixing (Figure 4c). There may be a substantial mixing in the MLCT states which when irradiated lead to interconversion to the LF state on Rh(III) responsible for photochemistry. If there is substantial Ru(II) character in the transitions in this region, the process involved is an intramolecular, energy-transfer process between two metal centers in the molecule.

Further work is ongoing to extend the threshold irradiation wavelength into the visible region of the spectrum and to attempt to determine the actual mechanism and states involved in the photochemistry and photophysics.

Conclusion

The monometallic dihydride complexes $RhH_2(PPh_3)_2L^+$ undergo photochemistry and photophysics from two different excited states. Photophysics occurs from an MLCT excited state generated by promoting a π-symmetry electron from Rh(III) into a π^* orbital on L. The photochemistry occurs from an LF state and is relatively independent of the nature of L.

When L is bpm, dpp, or dpq, a second $RhH_2(PPh_3)_2$ fragment can be bound to L to form a homonuclear, bimetallic complex, $[RhH_2(PPh_3)_2]_2L^{2+}$. The same type of LF photochemistry is observed for this bimetallic complexes as was observed for the monometallic species. However, room-temperature emission is not observed in this system due to the presence of a low-lying MLCT state, which efficiently deactivates the molecule back to the ground state.

Coupling the Rh(III) dihydride to a highly absorbing $Ru(bpy)_2$ fragment through bpm, dpp, or dpq results in the homonuclear, bimetallic complexes $(bpy)_2RuLRhH_2(PPh_3)_2^{3+}$. These complexes display photophysics characteristic of MLCT excited states associated with the Ru center and photochemistry characteristic of the LF state on the Rh center. The partitioning of the incident energy into processes that occur at different metal centers in these systems suggests that some intramolecular energy transfer is occurring in these systems. The wavelength dependence of the photochemistry also enables the approximation of the energy of the LF state responsible for photochemical H_2 production in these systems.

Acknowledgment. J.D.P. thanks the Office of Basic Energy Sciences, U.S. Department of Energy (DE-FG09-87ER13768), for support of this research and Johnson Matthey, Inc., for the loan of $RuCl_3$ and $RhCl_3$.

Contribution from the Discipline of Coordination Chemistry and Homogeneous Catalysis, Central Salt and Marine Chemicals Research Institute, Bhavnagar 364 002, India

Synthesis, Characterization, and EPR Studies of Stable Ruthenium(III) Schiff Base Chloro and Carbonyl Complexes

M. M. Taqui Khan,* D. Srinivas, R. I. Kureshy, and N. H. Khan

Received April 11, 1989

Stable ruthenium(III) carbonyl chelates of Schiff bases with axial ligands chloro, imidazole, and 2-methylimidazole are synthesized by interacting the methanolic solutions of their correspondng Ru(III) chloro complexes with carbon monoxide. The Schiff bases used are bis(salicylaldehyde) ethylenediimine (salen), bis(salicylaldehyde) *o*-phenylenediimine (saloph), bis(salicylaldehyde) diethylenetriimine (saldien), bis(picolinaldehyde) ethylenediimine (picen), bis(picolinaldehyde) *o*-phenylenediimine (picoph), and bis(picolinaldehyde) diethylenetriimine (picdien). These complexes are characterized by elemental analysis and IR, UV-visible, differential-pulse polarography, conductivity, magnetic susceptibility, and EPR techniques. The oxidation state of the metal ion in these complexes is confirmed to be +3 by electrochemical, magnetic susceptibility, and EPR measurements. The complexes belong to a low-spin Ru(III) $4d^5$ configuration. EPR studies indicate that the unpaired electron in the carbonyl complexes occupies the d_{xy} orbital. The distortion from the octahedral symmetry and delocalization parameters vary with the axial ligands, as well as with temperature. MO coefficients of T_2 orbitals in these complexes were estimated. A comparison of EPR results on chloro and carbonyl complexes is made. In the case of salen and saloph complexes, replacement of the axial ligand Cl^- by CO changes the energy level ordering. Differential-pulse polarographic study of the carbonyls reveals that the redox potential of Ru(III)/Ru(II) couple becomes more negative with increasing basicity of the axial ligand.

Introduction

Carbonyl complexes of transition-metal ions, especially those of ruthenium, are important in homogeneous catalysis of carbonylation and oxo reactions.[1-3] Much of the understanding about carbonyl complexes comes from the study of metal complexes in lower oxidation states[4] mainly due to the stabilization of these oxidation states by CO. Information on the higher valent carbonyls of ruthenium in aqueous solution is, however, restricted because of the hydrolytic tendencies of the metal ion in aqueous solution.[5,6]

(1) Süss-Fink, G.; Schmidt, G. F. *J. Mol. Catal.* **1987**, *42*, 361. Squarez, T.; Fontal, B. *Ibid.* **1985**, *32*, 191. Jenner, G.; Bitsi, G.; Schleiffer, E. *Ibid.* **1987**, *39*, 233.
(2) Taqui Khan, M. M.; Halligudi, S. B.; Abdi, S. H. R. *J. Mol. Catal.* **1988**, *44*, 179; Taqui Khan, M. M.; Halligudi, S. B.; Abdi, S. H. R. *Ibid.* **1988**, *45*, 215.
(3) Taqui Khan, M. M.; Halligudi, S. B.; Shukla, S. *Angew. Chem., Int. Ed. Engl.* in press.
(4) Schröder, M.; Stephenson, T. A. In *Comprehensive Coordination Chemistry*; Wilkinson, G., Ed.; Pergamon Press: New York, 1987; Vol. 4, Chapter 45, p 277.
(5) Taqui Khan, M. M.; Ramachandraiah, G.; Shukla, R. S. *Inorg. Chem.* **1988**, *27*, 3274.

0020-1669/90/1329-2320$02.50/0